*minerals*

MDPI

*Article*

# Bioadsorption of Terbium(III) by Spores of *Bacillus subtilis*

**Wei Dong [1,2,3], Huimin Wang [3], Zhoushen Ning [3], Kaijian Hu [3] and Xianping Luo [1,2,3,*]**

[1] National Innovation Center for Rare Earth Functional Material, Ganzhou 341000, China; wdong@jxust.edu.cn
[2] Jiangxi Key Laboratory of Mining and Metallurgy Environmental Pollution Control, Ganzhou 341000, China
[3] School of Resources and Environmental Engineering, Jiangxi University of Science and Technology, Ganzhou 341000, China; whmgzyx@163.com (H.W.); ningzhoushen@163.com (Z.N.); hukaijian@jxust.edu.cn (K.H.)
* Correspondence: luoxianping@jxust.edu.cn

**Abstract:** Wastewater containing low concentrations of rare earth ions not only constitutes a waste of rare earth resources but also threatens the surrounding environment. It is therefore necessary to develop environmentally friendly methods of recovering rare earth ions. The spores produced by *Bacillus* are resistant to extreme environments and are effective in the bioadsorption of rare earth ions, but their adsorption behaviors and mechanisms are not well understood. In this study, the cells and spores of *Bacillus subtilis* PS533 and PS4150 were used as biosorbents, and their adsorption of terbium ions was compared under different conditions. The adsorption characteristics of the spores were investigated, as were the possible mechanisms of interaction between the spores and rare earth ions. The results showed that the PS4150 spores had the best adsorption effect on Tb(III), with the removal percentage reaching 95.2%. Based on a computational simulation, SEM observation, XRD, XPS, and FTIR analyses, it was suggested that the adsorption of Tb(III) by the spores conforms to the pseudo−second−order kinetics and the Langmuir adsorption isotherm model. This indicates that the adsorption process mainly consists of chemical adsorption, and that groups such as amino, hydroxyl, methyl, and phosphate, which are found on the surface of the spores, are involved in the bioadsorption process. All of these findings suggest that *Bacillus subtilis* spores can be used as a potential biosorbent for the recovery of rare earth ions from wastewater.

**Keywords:** bioadsorption; *Bacillus subtilis*; spore; biosorbent; terbium(III); recovery



**Citation:** Dong, W.; Wang, H.; Ning, Z.; Hu, K.; Luo, X. Bioadsorption of Terbium(III) by Spores of *Bacillus subtilis*. *Minerals* **2022**, *12*, 866. https://doi.org/10.3390/min12070866

Academic Editor: Rajesh Kumar Jyothi

Received: 24 May 2022
Accepted: 5 July 2022
Published: 8 July 2022



## 1. Introduction

Rare earths are important strategic resources that are used around the world in the production of electronics, petrochemicals, machinery, and energy, as well as in smelting, the light industry, environmental protection, and agriculture. However, rare earth elements (REEs) have detrimental effects on the environment and on animals. Since the 1990s, REEs have been classified as a major pollutant [1]. Studies have shown that REEs can induce hormesis in animals, plants, and microorganisms, i.e., at low doses, REEs promote biological growth, with inhibitory or toxic effects occurring as the dose or concentration increases [2]. During mining and metallurgical processes, rare earth ions and their compounds inevitably enter the soil and water, thus damaging the surrounding soil and aquatic ecosystems; this not only affects the animals and plants in the area, but also has a negative impact on human health [3]. Therefore, the separation and recovery of REEs from the environment are very important, so that valuable resources can be recycled and for the protection of the environment.

Rare earth ions are difficult to separate from each other due to their similar chemical properties, ionic radii, and trivalent positive charge [4]. The complexity of this task, coupled with the demand for environmentally friendly technologies, is driving the development of biohydrometallurgy [5]. Compared with chemical precipitation, dissolution extraction, ion exchange, and membrane separation, biosorption is a more environmentally friendly,

efficient, and economical technique for the treatment and recovery of REEs [6]. This method commonly uses microorganisms for the adsorption of REEs, due to their large specific surface area, abundant sources, environmental friendliness, and low cost. Under acidic conditions, Bakers' yeast and *Penicillium* sp. show strong adsorption of neodymium, and the adsorbed amount is much higher than that of activated carbon [7]. The cell surface of *Penidiella* sp. can accumulate dysprosium in large quantities from mine wastewater [8]. *E. coli* and *Arthrobacter Nicotianae* exhibit high adsorption levels and can recover more than 90% of medium and heavy REEs from lignite leachate [9]. *Spirulina* powder can also be used as a biosorbent for the recovery of ytterbium from waste liquids, and has a maximum adsorption rate of 87.6% and a maximum adsorbed amount of 72.4 $mg \cdot g^{-1}$ [10].

Cells of the *Bacillus* species have a general adsorption effect on REEs. The adsorption rates of lanthanide and cerium ions by *Bacillus megaterium* cells were shown to be 29.2% and 30.2%, respectively [11]. *Bacillus licheniformis* can adsorb a variety of rare earth ions, including lanthanum, samarium, europium, gadolinium, and yttrium [12,13]. *Bacillus thuringiensis* shows strong capabilities in the adsorption of europium, terbium, and dysprosium ions [14]. Moreover, Tsuruta's results demonstrate that Gram−positive bacteria (e.g., *B. licheniformis* and *B. subtilis*) accumulated more Sm and Eu compared to actinomycetes, Gram−negative bacteria, fungi, and yeasts [13,15]. Previous studies have shown that *B. subtilis* cells can adsorb 17 REEs [4,13,16]. Spores are a type of dormancy formed by *Bacillus* in the absence of nutrients, but their structures are different from those of cells. *Bacillus* spores consist of an exosporium, a spore coat, an outer membrane, a peptidoglycan cortex, a germ cell wall, an inner membrane, and a core [17–19]. *B. subtilis* spores have no exosporium, and there is an electron−dense layer outside the spore coat, referred to by McKenney as the "crust" [20]. Compared to *Bacillus* cells, there are few studies on the adsorption of rare earth ions by spores. *Bacillus* spores are characterized by high-pressure resistance and rapid reproduction; they can survive at high temperatures, and under aerobic and even anaerobic conditions. *Bacillus* spores are highly resistant to harmful external factors and can also be used as effective biosorbents of REEs [5].

In this study, the strains *B. subtilis* PS533 and PS4150 were used to investigate the adsorption characteristics of rare earth ions in water. We examined the effects of various adsorption conditions, such as the biomass concentration, the initial concentration of rare earth ions, time, pH, and temperature, on the adsorption of Tb(III) by the cells and spores of the two bacteria. Isothermal adsorption and a kinetic analysis were performed via model fitting. The cells and spores of *B. subtilis* were also characterized and analyzed before and after adsorption to infer the possible mechanisms of adsorption occurrence; this provides a scientific basis for the separation and recovery of REEs in wastewater.

## 2. Materials and Methods

### *2.1. Bacterial Strains and the Preparation of Cells and Spores*

The bacterial strains *B. subtilis* PS533 and PS4150 were generously provided by Dr. Peter Setlow (UConn Health) and kept in our laboratory. Both strains are derived from wild-type strain *B. subtilis* PS832. The PS533 strain was inserted with the *Kar* gene and is therefore resistant to kanamycin. The PS4150 strain was inserted with the *tetR* and *spnR* genes, replacing the *cotE* and *gerE* genes; therefore, it is resistant to spectinomycin and has a highly defective spore surface that lacks most spore coat proteins [5,21].

The activated single colonies of PS533 and PS4150 were inoculated in a Luria−Bertani liquid medium with 1‰ kanamycin and 1‰ spectinomycin; then, they were incubated at 37 °C and 250 rpm until the logarithmic growth phase. The supernatant was removed after centrifugation, and the bacteria were washed three times with an appropriate amount of sterile water to obtain pure cells, which were then stored in the refrigerator at 4 °C.

During the logarithmic growth phase, the liquid cells of PS533 and PS4150 were coated on a 2× Schaeffer's−glucose solid (2× SG) medium with 1‰ kanamycin and 1‰ spectinomycin, and the bacteria on the surface of the medium were collected after 3~5 d of incubation at 37 °C. The collected bacteria were washed using sterile water and purified by

an ultrasonic cell crusher, removing the supernatant and the non−spore structures after centrifugation at 4 °C. The remaining material was suspended and kept in the refrigerator overnight at 4 °C. After repeating the previous step 3~4 times, the suspension was observed under a phase−contrast microscope to ensure that spores constituted at least 95%; it was then stored in a refrigerator at 4 °C for later use [18,22].

The precipitates obtained after the centrifugation of the suspended cells and spores were pre−cooled at −80°C for 6~8 h in an ultra-low temperature refrigerator, and then put into a vacuum freeze dryer for 24 h to dry into powder.

### *2.2. Adsorption of Tb(III) by B. subtilis*

The Tb(III) used here was terbium nitrate hexahydrate (Tb $(NO_3)_3 \cdot 6H_2O$; 99.9%) dissolved in sterile water. Rare earth ions can combine with 2,6-pyridinedicarboxylic acid (DPA) to form complexes, which produce fluorescence at specific wavelengths. Within a certain range, the intensity of this fluorescence has a significant linear relationship with the concentration of rare earth ions [5].

We investigated the effects of biomass concentration, the initial concentration of Tb(III), the pH, and the adsorption temperature on the adsorption performance of *B. subtilis*. A certain amount of the cells or spores were added to the solution that contained a given concentration of Tb(III); the solution was left for a period of time, and then centrifuged at 12,000 rpm for 2 min. Three replicates were set in each group. The fluorescence intensity of the rare earth ions in the solution was measured before and after adsorption by *B. subtilis*, and the concentration was calculated according to the Tb(III) concentration standard curve. The removal percentage $R$ (%) and the adsorbed amount $q_e$ (μmol $g^{-1}$) were calculated according to Equations (1) and (2), respectively:

$$R = \left(1 - \frac{C_e}{C_0}\right) \times 100 \quad (1)$$

$$q_e = (C_0 - C) \times V \div m \quad (2)$$

where $C_0$ is the concentration of rare earth ions in the solution before adsorption (μmol·$L^{-1}$), and $C_e$ is the concentration of rare earth ions in the solution after adsorption (μmol·$L^{-1}$). $V$ stands for the total volume of the adsorption solution (L), and $m$ for the mass of the cells or the spores (g).

### *2.3. Adsorption of Rare Earth Ions in Wastewater*

Soil from a mining area in Ganzhou, China, that contains rare earth elements was dried and ground. The soil was mixed with sterile water at a ratio of 1:1. After shaking, the supernatant was used as the experimental wastewater.

According to the adsorption steps described in Section 2.2, PS4150 spores were used to adsorb rare earth ions in the wastewater. The solution was filtered using a filter membrane before and after adsorption, and the content of rare earth elements was determined by inductively coupled plasma mass spectrometry (ICP-MS) (Angilent; 8800; Tokyo; Japan).

### *2.4. Characterization of B. subtilis Spores before and after Adsorption of Tb(III)*

Before and after adsorption of Tb(III), the PS4150 spores were turned into a powder using a vacuum freeze dryer; then, they were screened (pore size ≤ 75 μm) and collected for characterization.

After being sprayed gold, the micrographs of the samples were observed using SEM (FEI; MLA650F; Hillsboro, OR, USA). XRD (Bruker; D8 Advance; Karlsruhe; Germany) was used to detect the sample, and the scanning speed was 5° $min^{-1}$. All surface elements of the sample were analyzed using XPS (Thermo Fischer; ESCALAB 250Xi; Carlsbad; USA) with a passing energy of 20 eV and a step of 0.1 eV, and the charge correction was carried out with C1s = 284.8 eV binding energy as the energy standard. The surface functional

groups of the sample in the wave number range of 4000~400 $cm^{-1}$ were determined by FTIR (Shimadzu; Thermo Scientific Nicolet iS5; Kyoto; Japan), with a resolution of 4 $cm^{-1}$.

## 3. Results

### *3.1. Effects of Adsorption Conditions on Tb(III) Adsorption*

The increased addition of cells or spores had an important effect on the amounts of rare earth ions that were adsorbed. When the amount of the cells and spores that were added was increased, the percentage of Tb(III) removed by the cells and spores of the two tested strains also increased (Figure 1a). The biomass concentration increases the adsorption sites, meaning that the adsorption effect of rare earth ions is enhanced by cells and spores in a certain range [23]. When the biomass concentration was 2 $g \cdot L^{-1}$, the trend in the increase in the percentage of Tb(III) removed by the two strains tended to be flat. If more cells or spores were added, the active sites of the biosorbents interfered with each other, and the amount adsorbed per unit of biosorbent decreased [24]. Therefore, it was determined that the optimum biomass concentration was 2 $g \cdot L^{-1}$.

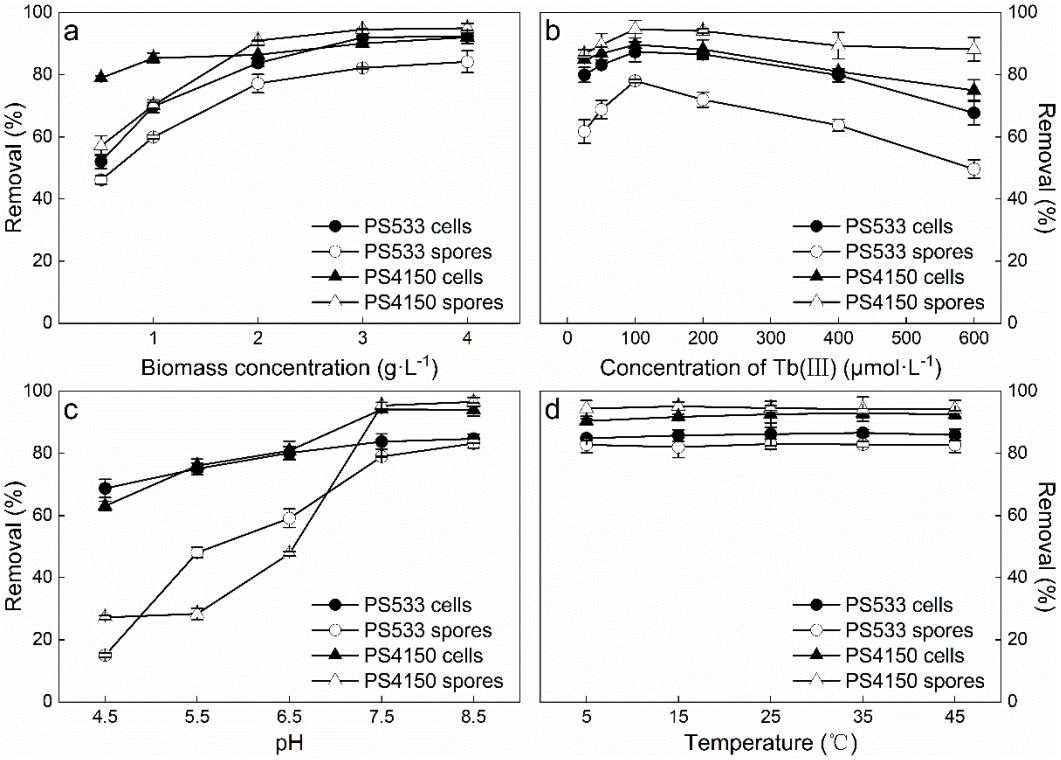


**Figure 1.** Tb(III)−removal by *B. subtilis* PS533/PS4150 cells and spores under different conditions: (**a**) biomass concentration (0.5~3 $g \cdot L^{-1}$), (**b**) initial concentration of Tb(III) (25~600 $\mu mol \cdot L^{-1}$), (**c**) pH (4.5~8.5), and (**d**) temperature (5~45 °C).

Figure 1b shows the influence of the initial concentration of Tb(III) on the adsorption effect. The results illustrate that the increase in the initial concentration of Tb(III) was accompanied by an increase in the removal percentage, which peaked at 100 $\mu mol \cdot L^{-1}$. The PS4150 spores had the highest removal percentage, removing 94.7% of the Tb(III). When the initial concentration of Tb(III) exceeded 100 $\mu mol \cdot L^{-1}$, the removal percentage tended to decrease instead. This might be because the adsorption sites on the surface of the bacteria are limited. As the concentration of rare earth ion increases, the adsorption sites are fully utilized, and the adsorption gradually reaches saturation. When there are not enough effective adsorption sites to bind the remaining rare earth ions, the removal percentage decreases continuously. However, at the same time, rare earth ions can induce hormesis in microorganisms [2]. At increased concentrations, rare earth ions become increasingly toxic

to microorganism, reducing the biological activity of microorganisms, and resulting in a decreased removal percentage. Accordingly, when the initial concentration of Tb(III) was 100 μmol·$L^{-1}$, the bacterial adsorption and removal effect of Tb(III) was better.

From Figure 1c, it is clear that pH had a significant influence on the bacteria's adsorption of Tb(III). When the pH was acidic, the removal rate of Tb(III) by the bacteria was low. This is consistent with the conclusions of other studies on *Bacillus* [5,14,25]. The removal rate of Tb(III) by spores showed a more obvious change, increasing rapidly with the increase in pH. It is likely that, with the increase in the pH value, functional groups such as phosphates on the spore surface are deprotonated, cations are reduced, and negative charges are increased; meanwhile, rare earth ions still exist in the form of positive electricity, enhancing the electrostatic interaction and complexation between spores and rare earth ions, and increasing the removal rate of Tb(III) [26,27]. When the pH was 7.5, the percentage of Tb(III) removed by the spores reached equilibrium. Thus, the two strains are more suitable for adsorbing Tb(III) in neutral or weak alkaline environments.

Different microorganisms' tolerances to temperature ranges widely, and the temperature of the solution may affect the activity of microorganisms and the migration of rare earth ions [28]. In this study, the adsorption temperature had no significant effect on the adsorption of Tb(III) by PS533 and PS4150 cells or spores, and the removal percentage changed little within the range of 5~45 °C (Figure 1d). This may be due to the adaptability of *B. subtilis* to the environment and its wide range of temperature tolerance.

### *3.2. Biosorption Effect of Spores on Actual Wastewater*

Wastewater usually contains a mixture of different metal ions. The matter of whether a biosorbent can selectively adsorb the rare earth ions in the mixed rare earth ion solution is an important index for evaluating the performance of the biosorbent. The leaching solution of soil in a rare earth mining area was taken as the research object. There were differing amounts of each rare earth element in the leaching solution with more Y, Tb, and Pr, and less La, Nd, Dy, Er, and Yb; meanwhile, the amount of other rare earth elements was less than 0.1 ppb. After adsorption by the PS4150 spores, the contents of the other rare earth elements, except Pr, were less than 0.1 ppb (Figure 2). This demonstrates that the spores of *B. subtilis*, especially PS4150, have a practical significance for the separation and recovery of rare earth ions from wastewater.

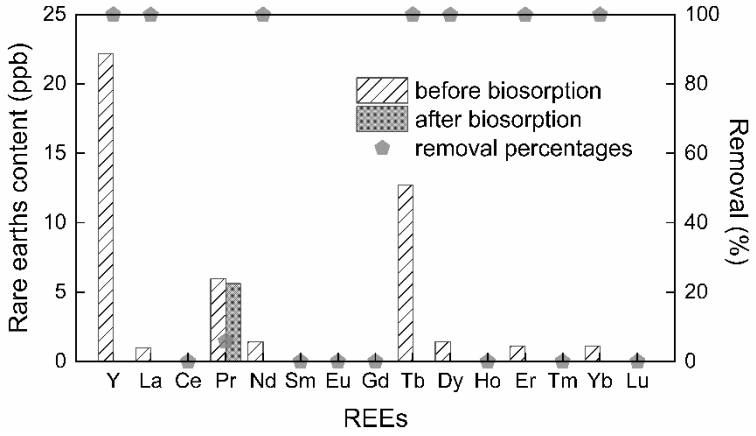


**Figure 2.** The content of REEs in soil leaching solution of rare earth mining area before and after the biosorption by PS4150 spores.

### *3.3. Kinetic Study of Tb(III) Adsorption*

The effects of different contact times on the adsorption of Tb(III) by PS533 and PS4150 cells and spores were tested at room temperature, with a biomass concentration of 2 g·$L^{-1}$, and an initial concentration of Tb(III) of 100 μmol $L^{-1}$. The results are shown in Figure 3a. The processes by which rare earth ions are adsorbed by biosorbents can be divided into

two general phases: rapid adsorption, and a slow increase that gradually reaches equilibrium [29,30]. Within the timeframe 0~30 min, the amount of Tb(III) adsorbed by the cells and spores increased continuously over time, and reached a stable level at 30 min. Even if the contact time was prolonged, there was little change in the amount adsorbed.

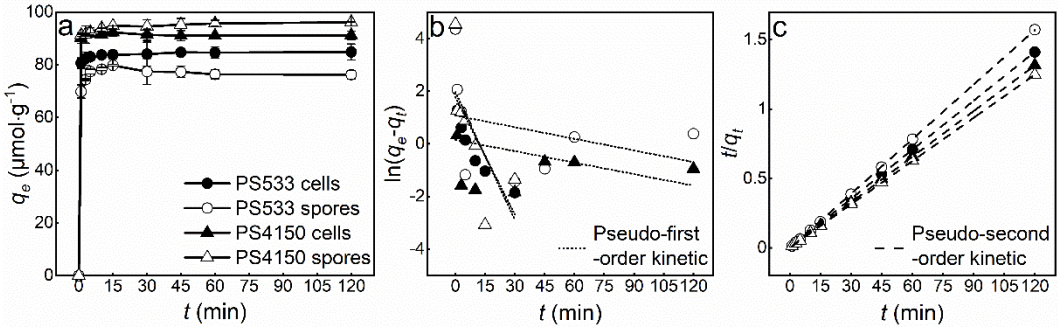


**Figure 3.** (**a**) The amount of Tb(III) adsorbed by *B. subtilis* PS533/PS4150 cells and spores were related to the contact time; (**b**) Pseudo−first−order kinetic model fitting; (**c**) Pseudo−second−order kinetic model fitting.

The increase in the amount adsorbed may be explained by the rapid adsorption of Tb(III) to the adsorption sites of the bacteria due to the coordination reaction between rare earth ions and the coordination groups on the bacterial surface during the initial adsorption. As the adsorption time increases, the adsorption sites have been fully utilized. Therefore, it is necessary to determine the appropriate adsorption time needed to reach equilibrium, not only to maintain a high level of adsorption, but also to save as much time as possible. The results show that an adsorption time of 30 min would be sufficient.

In order to study the mechanisms by which *B. subtilis* absorbs Tb(III), pseudo−first−order Equation (3) and pseudo−second−order Equation (4) adsorption kinetic models were used to fit the experimental data:

$$\ln(q_e - q_t) = \ln q_e - K_1 t \quad (3)$$

$$t/q_t = 1/K_2 q_e^2 + t/q_e \quad (4)$$

where $q_e$ and $q_t$ represent the amount (μmol·g$^{-1}$) of Tb(III) adsorbed on the biosorbent at equilibrium and time $t$, respectively. $K_1$ and $K_2$ are pseudo−first−order and pseudo−second−order adsorption rate constants, respectively.

The adsorption kinetics reflect the variation in the amount adsorbed over time. The equilibrium time for Tb(III) adsorption by PS533 and PS4150 cells and spores was short, ranging from 15 to 30 min, which demonstrates the significant economic benefits of these biosorbents. The pseudo−first−order kinetic model assumes that adsorption is controlled by diffusion steps, but the estimation is ambiguous due to the slow dynamics of the process caused by a weak van der Waals force or intragranular diffusion [31]. The pseudo−second−order kinetic model is mostly used to describe adsorption processes dominated by chemical adsorption (i.e., ion exchange or complexation), and most biosorption kinetics follow pseudo−second−order adsorption kinetics [32].

According to the parameters of the fitting results (Table 1), the correlation coefficients ($R^2$) of the pseudo−second−order kinetic model were >0.99, and the fitted adsorption amount differed very little from the actual equilibrium amount in the experiment. The adsorption kinetics of Tb(III) by cells and spores conformed to the pseudo−second−order kinetics model (Figure 3c), indicating that it is an adsorption process dominated by chemical adsorption.

**Table 1.** Adsorption kinetic model parameters of Tb(III) by *B. subtilis*.

| Different Biosorbents | Amount Adsorbed/ (μmol·g$^{-1}$) † | Pseudo–First–Order Kinetic | | | Pseudo–Second–Order Kinetic | | |
|---|---|---|---|---|---|---|---|
| | | $K_1$ | $q_e$/(μmol·g$^{-1}$) | $R^2$ | $K_2$ | $q_e$/(μmol·g$^{-1}$) | $R^2$ |
| PS533 cells | 83.865 | −0.149 | 5.956 | 0.510 | 0.081 | 84.962 | 0.999 |
| PS533 spores | 79.790 | −0.015 | 2.930 | −0.050 | 0.054 | 76.220 | 0.999 |
| PS4150 cells | 92.326 | −0.015 | 1.171 | −0.070 | 0.286 | 91.158 | 0.999 |
| PS4150 spores | 94.792 | −0.162 | 7.162 | 0.422 | 0.041 | 96.246 | 0.999 |

† The data shown are average values.

### 3.4. Isotherm Study of Tb(III) Adsorption

The PS533 and PS4150 cells and spores were used to adsorb different concentrations of Tb(III) at 25 °C for 30 min. The adsorbed amount increased rapidly with the increase in the Tb(III) concentration, and then tended to stabilize. The experimental results were fitted by two common adsorption isotherm models, the Langmuir isotherm Equation (5) and Freundlich isotherm Equation (6), which are shown here:

$$q_e = q_{max} K_L C_e / (1 + K_L C_e) \quad (5)$$

$$q_e = K_F C_e^{1/n} \quad (6)$$

where $q_e$ is the amount absorbed at equilibrium (μmol·g$^{-1}$), $C_e$ is the concentration of the Tb(III) solution at equilibrium (μmol·L$^{-1}$), $q_{max}$ is the fitted single-layer maximum adsorbed amount (μmol·g$^{-1}$), $K_L$ is the Langmuir adsorption correlation constant, and $K_F$ and $n$ are the Freundlich adsorption correlation constants.

Table 2 shows the fitting parameters of the adsorption isotherm of Tb(III) adsorbed by *B. subtilis* cells and spores. The adsorption processes were more in line with the Langmuir adsorption isotherm model (Figure 4b). The theoretical maximum adsorbed amounts of the four biosorbents were 857.1, 495.9, 1171.2, and 1557.2 μmol·g$^{-1}$, respectively. Similar to the higher removal percentage, the maximum adsorption capacity of PS4150 was the highest. This shows that the adsorption of Tb(III) by *B. subtilis* should be a reversible adsorption process, with uniform adsorption sites on the surface of the biosorbents [33,34]. It is also evident that the parameter $1/n$ of the Freundlich isotherm model is between 0~1, indicating that the adsorption is efficient over the entire range of concentrations studied, and that a strong bond is formed between the biosorbent and rare earth ions [35,36].

**Table 2.** Adsorption isotherm model parameters of Tb(III) by *B. subtilis*.

| Different Biosorbents | Langmuir Isotherm | | | Freundlich Isotherm | | |
|---|---|---|---|---|---|---|
| | $q_{max}$ (μmol·g$^{-1}$) | $K_L$ | $R^2$ | $1/n$ | $K_F$ | $R^2$ |
| PS533 cells | 857.140 | 0.001 | 0.995 | 0.460 | 19.145 | 0.939 |
| PS533 spores | 495.850 | 0.002 | 0.993 | 0.395 | 20.213 | 0.909 |
| PS4150 cells | 1 171.200 | 0.001 | 0.991 | 0.507 | 16.763 | 0.944 |
| PS4150 spores | 1 557.208 | 0.001 | 0.990 | 0.542 | 15.913 | 0.950 |

### 3.5. Characterization of Spores before and after Adsorption

Taking the spores of *B. subtilis* PS4150 as an example, the mechanisms whereby rare earth ions are adsorbed by the spores were characterized.

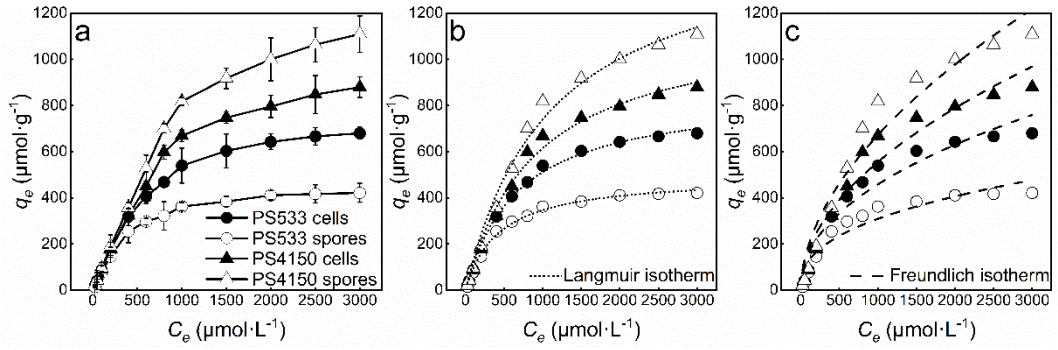


**Figure 4.** (**a**) The amount of Tb(III) adsorbed by *B. subtilis* PS533/PS4150 cells and spores were related to the concentration of Tb(III); (**b**) Langmuir isotherm model fitting; (**c**) Freundlich isotherm model fitting.

The morphological changes in spores before and after the adsorption of Tb(III) were observed using a scanning electron microscope (SEM). The spores were oval shaped, and there were some deposits on their surfaces after adsorption of Tb(III) (Figure 5b,e). This may be due to the adsorption and precipitation of rare earth ions on the spore's surface. After adsorption, the spore structure was complete, indicating that Tb(III) was only adsorbed on the surface of the spore and did not penetrate the internal structure. The elemental composition of the spores before and after their adsorption of Tb(III) was analyzed by EDS, and the results are shown in Figure 5c,f and Table 3. The surface elements of the spores are mainly C and O, and small amounts of Mg, P, S, Ca, and Mn. These minor elements are derived from the 2× SG medium. After adsorption, the elemental mass percentage of Tb(III) on the surfaces of the PS533 and PS4150 spores increased from 0% to 0.81% and 1.38%, respectively, which confirmed both the biosorption of Tb(III) on the surface of the spores, and that PS4150 had adsorbed more. These results reflect the fact that the spore adsorption effects of PS533 and PS4150 are different. The results also show that the surfaces of spores play an important role in the adsorption of rare earth ions [37]. After adsorption, the mass percentages of Ca and Mn decreased, indicating that there is also ion exchange in the process of spore adsorption of Tb(III).

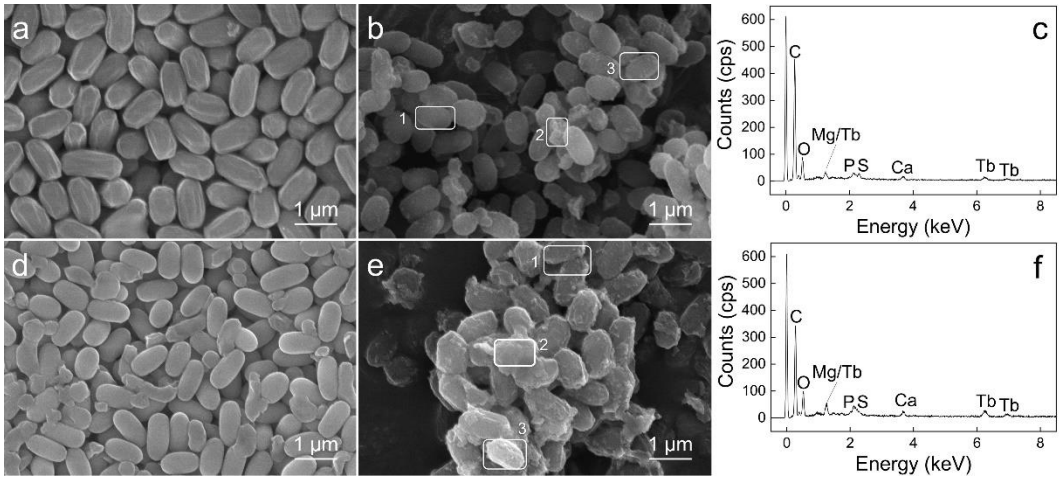


**Figure 5.** SEM micrographs of (**a**) PS533 spores, (**b**) PS4150 spores, (**d**) PS533 spores−Tb, and (**e**) PS4150 spores−Tb. EDS spectrum of (**c**) PS533 spores−Tb and (**f**) PS4150 spores−Tb. Counts results are calculated from the average of the energy intensities of the three regions of the spore after adsorption.

**Table 3.** Elemental mass percentage of *B. subtilis* spores before and after the adsorption of Tb(III).

| Different Biosorbents | Elemental Mass Percentage (%) | | | | | | | |
|---|---|---|---|---|---|---|---|---|
| | C | O | Mg | P | S | Ca | Mn | Tb |
| PS533 spores | 74.35 | 20.24 | 0.22 | 1.18 | 1.07 | 2.84 | 0.10 | 0.00 |
| PS533 spores-Tb | 74.93 | 23.25 | 0.26 | 0.09 | 0.18 | 0.48 | 0.00 | 0.81 |
| PS4150 spores | 73.27 | 21.00 | 0.41 | 0.93 | 1.05 | 3.13 | 0.21 | 0.00 |
| PS4150 spores-Tb | 72.01 | 24.94 | 0.59 | 0.09 | 0.19 | 0.80 | 0.00 | 1.38 |

The mass percentages shown are average values.

According to the survey scanning spectra of the spores (Figure 6a), the elemental composition of the spore surface mainly comprised C, N, and O. After adsorption, the binding energies of Tb 3d3 and Tb 3d5 appeared at 1240.84 eV and 1276.15 eV, respectively (Figure 6b), indicating that Tb ions exist in a trivalent state on the surface of the spores, and that no redox reaction occurs during the adsorption process [38]. After adsorption, the peaks of the elements O, C, and N increased, indicating that the functional groups related to these elements may play a role in adsorption.

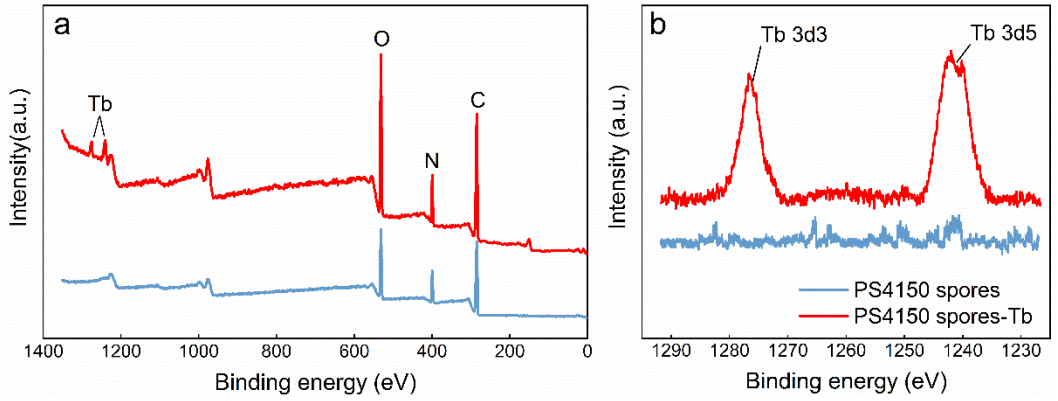


**Figure 6.** XPS spectrum of spores before and after adsorption of Tb(III): (**a**) survey scanning spectra; (**b**) Tb 3d spectra of Tb−spores.

The FTIR spectra of the spores before and after adsorption of Tb(III) were measured at wave numbers in the range of 400~4000 $cm^{-1}$ (Figure 7). The strong broad spectrum peak at 3300 $cm^{-1}$ is the stretching vibration peak of O−H and C−H of fatty acids; this range also encompasses the stretching vibration absorption of the N–H bond from protein molecules [39]. The absorption peak at 2962~2854 $cm^{-1}$ is the C−H stretching vibration peak. The peaks at 2930 and 2962 $cm^{-1}$ are the asymmetrical stretching vibration peaks of the $-CH_2$ and $-CH_3$ groups of proteins and lipids, respectively. It is a typical stretching vibration absorption band of C−H bonds of the lipid carbon chain. It reflects the information of the fatty acids, various membranes, and other structural hydrophilic lipid molecules [40]. The peaks at 1656 $cm^{-1}$ and 1543 $cm^{-1}$ are from the C=O stretching vibration peak of the protein amide I band, and the N−H in-plane bending vibration and C−N stretching vibration of the protein amide II band. The absorption bands around 1442 $cm^{-1}$ and 1383 $cm^{-1}$ belong to the symmetrical deformation vibration peaks of the methyl groups in the protein molecules. The absorption peak at 1280 $cm^{-1}$ is the C−H stretching vibration of the aliphatic carbon chain. The wavenumber range of 1200~900 $cm^{-1}$ contains a wide band of carbohydrates and phosphodiesters [39,41]. The peaks at 1239 $cm^{-1}$ and 1080 $cm^{-1}$ are the out-of-plane bending vibration peaks of phosphate groups in the carbohydrates. The absorption of 1160 $cm^{-1}$ comes from the stretching vibration of the C−O bond in the polysaccharides. The absorption band at 900~700 $cm^{-1}$ is the "fingerprint area", because it contains a weak but very unique absorbance, which is unique to specific bacteria [42]. The absorption band of 770~660 $cm^{-1}$ is generally the range of the out−of−plane bending

of the C−H bond in polysaccharides. However, several studies have suggested that the absorption band here is due to the presence of DPA [41,43,44]. DPA in spores chelates with $Ca^{2+}$ and exists in the form of calcium salt. It constitutes as much as 20% of the dry weight of the spore's core [45]. Ca−DPA is also found in the outer layers of the spore (such as the cortex and coat layer).

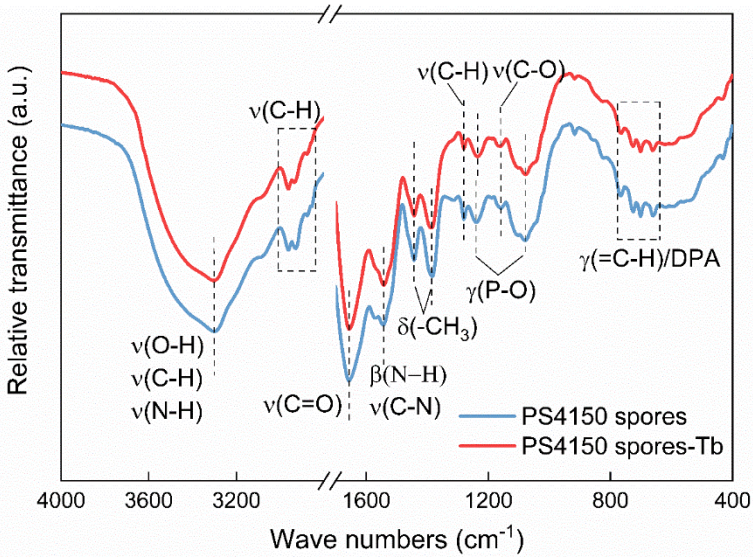


**Figure 7.** FTIR spectrum of spores before and after adsorption of Tb(III).

The shape of the peak in the infrared spectrum after adsorption was basically consistent with the shape detailed above, indicating that the main components and structure of PS4150 spores remained intact after adsorption. However, the wave numbers of some groups on the spores shifted, including amino and hydroxyl (3300 → 3302 $cm^{-1}$), methyl (1383 → 1386 $cm^{-1}$), and phosphate (1239 → 1235 $cm^{-1}$, 1080 → 1078 $cm^{-1}$), indicating that these groups participate in the adsorption of, and form complexes with, rare earth ions. These results further indicate that the adsorption mainly occurs on the surface of the spores.

## 4. Discussion

Although microbial cells have attracted much attention from researchers investigating methods for the removal of rare earth ions from water or wastewater, they require high amounts of nutrition and a favorable environment to support their growth and bioadsorption functions. In this paper, the cells and spores of *B. subtilis* were used as biosorbents to adsorb Tb(III) in a solution containing a certain concentration of Tb(III); this experiment simulated the recovery and removal of rare earth ions in wastewaters. The adsorption effects of the cells and spores of PS533 and PS4150 on rare earth ions were compared, and the effects under different conditions were explored. The removal percentage of Tb(III) by the PS4150 spores was the highest. This might be because of the lack of the spore coat protein *cotE* in PS4150, a gene-deficient strain, which causes the spores to lose the inner coat layer and most of the outer coat layer, meaning that more rare earth ions can be adsorbed and accumulated on the surface. The adsorption capacity of Tb(III) by the spores was at its the highest with a biomass concentration of 2 $g \cdot L^{-1}$, an initial concentration of Tb(III) of 100 $\mu mol \cdot L^{-1}$, a pH of 7.5, and an adsorption duration of 30 min. The percentage of Tb(III) removed by the PS4150 spores was about 94%, and the adsorbed amount was about 93 $\mu mol \cdot g^{-1}$.

The adsorption of rare earth ions by *Bacillus* cells usually occurs on the cell wall, and the main adsorption sites are the carboxyl, hydroxyl, and phosphate groups [12,46,47]. The adsorption of light REEs and medium REEs is dominated by phosphoric acid groups, while the adsorption of some medium and heavy REEs is mainly coordinated by carboxyl

groups [48]. Some rare earth ions are also adsorbed to the cell membrane or periplasmic space, or accumulate inside the cells [49]. However, there are few studies on the binding sites of rare earth ions on the spores. One previous study shows that the adsorption of rare earth ions occurs on the outer layer of the spores, but it might also be affected by the spores' internal mechanisms [5]. The specific structures, components, and mechanisms by which spores bind to rare earth ions are not clear and need to be further studied.

The pseudo-second-order kinetic model is generally used to predict the adsorption behavior of solid biosorbents. It is assumed that the chemical adsorption mechanism is the rate-limiting aspect of the whole adsorption process [50], and that the resistance of mass transfer usually occurs in the outer layer of the biosorbent [51]. The adsorption processes of biosorbents mostly conform to the pseudo-second-order chemical reaction kinetic model, while the pseudo-order adsorption kinetic model is only in good agreement with the experimental data in the initial stage of the first step reaction [32,52]. Our results also align with this finding. The Langmuir and Freundlich adsorption isotherm models are widely used to describe the adsorption of rare earth ions by biosorbents; of these, Langmuir proves to be a better fit for most of the adsorption [52]. The Langmuir isotherm assumes that the adsorption is a monolayer adsorption on the surface of a homogeneous biosorbent [53]. However, the biosorbent surface is not ideally homogeneous. Regarding the actual adsorption, the combination of the Langmuir and Freundlich models can better explain the adsorption mechanism. The results of our fitting show that the $R^2$ of the Langmuir model is more than 0.99 and that the $R^2$ of the Freundlich model is also between 0.90~0.95. The adsorption mechanism under consideration here may exhibit behaviors somewhere between those of monolayer adsorption mechanisms and those of multilayer adsorption mechanisms [6]. This is the result of chemical action and weak physical force; the rare earth ions cover the biosorbent surface through ion complexation, electrostatic action, precipitation, and other actions [31].

Spores of *B. subtilis* can quickly adsorb rare earth ions in tens of minutes; the process is especially quick in a liquid state. Lipoteichoic acid and wall teichoic acid of the *Bacillus* cells are the main cation adsorption sites [16,54]. Although teichoic acid is not present in *Bacillus* spores, the outer layer may contain large amounts of excess phosphate [5]. In a process similar to that of *Bacillus* cells, adsorption mainly occurs on the surface of spores. Proteins and carbohydrates in the outer coat layer form a matrix around the spore coat proteins [55]. Due to electrostatic attraction, rare earth ions gather on charged points on the spore's surface and replace the Ca and Mn ions that were originally fixed to these charged points. The amino, hydroxyl, methyl, and phosphate groups on the spore coat layer participate in the adsorption process, and in complex with Tb(III), form amorphous compounds on the spore surface.

According to our findings, *B. subtilis* spores can adsorb a large amount of Tb(III) in neutral environments, and the amount adsorbed can theoretically reach 1,557.2 $\mu mol \cdot g^{-1}$. Moreover, spores of the *Bacillus* species are highly tolerant to extreme environments. Therefore, *B. subtilis* spores could be used as potential biosorbents for the removal or recovery of rare earth ions from wastewater.

**Author Contributions:** Conceptualization, methodology, writing—review and modification, W.D.; experiment, data curation, and writing—original draft preparation, H.W.; experiment and data curation, Z.N.; conceptualization and revision, K.H.; materials and review, X.L. All authors have read and agreed to the published version of the manuscript.

**Funding:** This work was supported by the Natural Science Foundation of China (No. 92062110, 51904119), the Jiangxi Provincial Natural Science Foundation (No. 20212ACB213004), and the Science and Technology Program of Ganzhou (No. 202101095076).

**Acknowledgments:** The authors gratefully acknowledge Peter Setlow for his suggestions to this work, and Wei Dong would like to thank the Youth Jinggang Scholars Program in Jiangxi Province (No. QNJG2020050).

**Conflicts of Interest:** The authors declare no conflict of interest.

## References


1. Wei, Z.; Hong, F.; Yin, M.; Li, H.; Hu, F.; Zhao, G.; WoonchungWong, J. Subcellular and molecular localization of rare earth elements and structural characterization of yttrium bound chlorophyll a in naturally grown fern *Dicranopteris dichotoma*. *Microchem. J.* **2005**, *80*, 1–8. [CrossRef]
2. Pagano, G.; Guida, M.; Tommasi, F.; Oral, R. Health effects and toxicity mechanisms of rare earth elements—Knowledge gaps and research prospects. *Ecotoxicol. Environ. Saf.* **2015**, *115*, 40–48. [CrossRef]
3. Guo, G.L.; Zhou, Q.X. Evaluation of heavy metal contamination in Phaeozem of northeast China. *Environ. Geochem. Health* **2006**, *28*, 331–340. [CrossRef]
4. Park, D.M.; Reed, D.W.; Yung, M.C.; Eslamimanesh, A.; Lencka, M.M.; Anderko, A.; Fujita, Y.; Riman, R.E.; Navrotsky, A.; Jiao, Y. Bioadsorption of rare earth elements through cell surface display of lanthanide binding tags. *Environ. Sci. Technol.* **2016**, *50*, 2735–2742. [CrossRef]
5. Dong, W.; Li, S.; Camilleri, E.; Korza, G.; Yankova, M.; King, S.M.; Setlow, P. Accumulation and release of rare earth ions by spores of *Bacillus* species and the location of these ions in spores. *Appl. Environ. Microbiol.* **2019**, *85*, e00956–e01019. [CrossRef]
6. Sadovsky, D.; Brenner, A.; Astrachan, B.; Asaf, B.; Gonen, R. Biosorption potential of cerium ions using *Spirulina* biomass. *J. Rare Earths* **2016**, *34*, 644–652. [CrossRef]
7. Palmieri, M.C.; Garcia, O.; Melnikov, P. Neodymium biosorption from acidic solutions in batch system. *Process. Biochem.* **2000**, *36*, 441–444. [CrossRef]
8. Horiike, T.; Yamashita, M. A new fungal isolate, *Penidiella* sp. strain T9, accumulates the rare earth element dysprosium. *Appl. Environ. Microbiol.* **2015**, *81*, 3062–3068. [CrossRef]
9. Park, D.; Middleton, A.; Smith, R.; Deblonde, G.; Laudal, D.; Theaker, N.; Hsu-Kim, H.; Jiao, Y. A biosorption-based approach for selective extraction of rare earth elements from coal byproducts. *Sep. Purif. Technol.* **2020**, *241*, 116726. [CrossRef]
10. Shu, Q.; Liao, C.; Zou, W.; Xu, B.; Tan, Y. Recovery of rare earth element ytterbium(III) by dried powdered biomass of *spirulina*: Adsorption isotherm, kinetic and thermodynamic study. *Trans. Nonferrous Met. Soc. China* **2021**, *31*, 1127–1139. [CrossRef]
11. Zheng, C.; Wang, Y.; Chen, M.; Jiang, Z.; Yang, L.; Zhang, X. Interactions between *Bacillus megaterium* and rare earth ions. *Chin. Rare Earths* **2016**, *37*, 132–136. [CrossRef]
12. Cheng, Y.; Zhang, L.; Bian, X.; Zuo, H.; Dong, H. Adsorption and mineralization of REE-lanthanum onto bacterial cell surface. *Environ. Sci. Pollut. Res.* **2018**, *25*, 22334–22339. [CrossRef]
13. Tsuruta, T. Accumulation of rare earth elements in various microorganisms. *J. Rare Earths* **2007**, *25*, 526–532. [CrossRef]
14. Pan, X.; Wu, W.; Lü, J.; Chen, Z.; Li, L.; Rao, W.; Guan, X. Biosorption and extraction of europium by *Bacillus thuringiensis* strain. *Inorg. Chem. Commun.* **2017**, *75*, 21–24. [CrossRef]
15. Tsuruta, T. Selective accumulation of light or heavy rare earth elements using gram-positive bacteria. *Colloid Surf. B* **2006**, *52*, 117–122. [CrossRef]
16. Takahashi, Y.; Chatellier, X.; Hattori, K.H.; Kato, K.; Fortin, D. Adsorption of rare earth elements onto bacterial cell walls and its implication for REE sorption onto natural microbial mats. *Chem. Geol.* **2005**, *219*, 53–67. [CrossRef]
17. Qin, H.; Driks, A. Contrasting evolutionary patterns of spore coat proteins in two *Bacillus* species groups are linked to a difference in cellular structure. *BMC Evol. Biol.* **2013**, *13*, 261. [CrossRef]
18. Setlow, P. Observations on research with spores of *Bacillales* and *Clostridiales* species. *J. Appl. Microbiol.* **2019**, *126*, 348–358. [CrossRef]
19. Setlow, P. Spore germination. *Curr. Opin. Microbiol.* **2003**, *6*, 550–556. [CrossRef]
20. McKenney, P.T.; Driks, A.; Eskandarian, H.A.; Grabowski, P.; Guberman, J.; Wang, K.H.; Gitai, Z.; Eichenberger, P. A distance-weighted interaction map reveals a previously uncharacterized layer of the *Bacillus subtilis* spore coat. *Curr. Biol.* **2010**, *20*, 934–938. [CrossRef]
21. Ghosh, S.; Setlow, B.; Wahome, P.G.; Cowan, A.E.; Plomp, M.; Malkin, A.J.; Setlow, P. Characterization of spores of *Bacillus subtilis* that lack most coat layers. *J. Bacteriol.* **2008**, *190*, 6741–6748. [CrossRef]
22. Dong, W.; Green, J.; Korza, G.; Setlow, P. Killing of spores of *Bacillus* species by cetyltrimethylammonium bromide. *J. Appl. Microbiol.* **2019**, *126*, 1391–1401. [CrossRef]
23. Wang, L.; Wan, C.; Zhang, Y.; Lee, D.-J.; Liu, X.; Chen, X.; Tay, J.-H. Mechanism of enhanced Sb(V) removal from aqueous solution using chemically modified aerobic granules. *J. Hazard. Mater.* **2015**, *284*, 43–49. [CrossRef]
24. Iftekhar, S.; Srivastava, V.; Ben Hammouda, S.; Sillanpaa, M. Fabrication of novel metal ion imprinted xanthan gum-layered double hydroxide nanocomposite for adsorption of rare earth elements. *Carbohydr. Polym.* **2018**, *194*, 274–284. [CrossRef]
25. Naskar, A.; Guha, A.K.; Mukherjee, M.; Ray, L. Adsorption of nickel onto *Bacillus cereus* $M^1{}_{16}$: A mechanistic approach. *Sep. Sci. Technol.* **2016**, *51*, 427–438. [CrossRef]
26. Di, T.; Tan, D.; Yu, Q.; Lin, J.; Zhu, T.; Li, T.; Li, L. Ultra-high performance of hyper-crosslinked phosphate-based polymer for uranium and rare earth element adsorption in aqueous solution. *Langmuir* **2019**, *35*, 13860–13871. [CrossRef]
27. Bhattacharya, A.K.; Naiya, T.K.; Mandal, S.N.; Das, S.K. Adsorption, kinetics and equilibrium studies on removal of Cr(VI) from aqueous solutions using different low-cost adsorbents. *Chem. Eng. J.* **2008**, *137*, 529–541. [CrossRef]

28. Iftekhar, S.; Ramasamy, D.L.; Srivastava, V.; Asif, M.B.; Sillanpää, M. Understanding the factors affecting the adsorption of lanthanum using different adsorbents: A critical review. *Chemosphere* **2018**, *204*, 413–430. [CrossRef]
29. Ashour, R.M.; El-sayed, R.; Abdel-Magied, A.F.; Abdel-khalek, A.A.; Ali, M.M.; Forsberg, K.; Uheida, A.; Muhammed, M.; Dutta, J. Selective separation of rare earth ions from aqueous solution using functionalized magnetite nanoparticles: Kinetic and thermodynamic studies. *Chem. Eng. J.* **2017**, *327*, 286–296. [CrossRef]
30. Zhou, Q.; Yang, H.; Yan, C.; Luo, W.; Li, X.; Zhao, J. Synthesis of carboxylic acid functionalized diatomite with a micro-villous surface via UV-induced graft polymerization and its adsorption properties for lanthanum(III) ions. *Colloids Surf. A* **2016**, *501*, 9–16. [CrossRef]
31. Gupta, N.K.; Gupta, A.; Ramteke, P.; Sahoo, H.; Sengupta, A. Biosorption-a green method for the preconcentration of rare earth elements (REEs) from waste solutions: A review. *J. Mol. Liq.* **2019**, *274*, 148–164. [CrossRef]
32. Ho, Y.S.; McKay, G. Pseudo-second order model for sorption processes. *Process. Biochem.* **1999**, *34*, 451–465. [CrossRef]
33. Fan, T.; Liu, Y.; Feng, B.; Zeng, G.; Yang, C.; Zhou, M.; Zhou, H.; Tan, Z.; Wang, X. Biosorption of cadmium(II), zinc(II) and lead(II) by *Penicillium simplicissimum*: Isotherms, kinetics and thermodynamics. *J. Hazard. Mater.* **2008**, *160*, 655–661. [CrossRef]
34. Alshameri, A.; He, H.; Xin, C.; Zhu, J.; Xinghu, W.; Zhu, R.; Wang, H. Understanding the role of natural clay minerals as effective adsorbents and alternative source of rare earth elements: Adsorption operative parameters. *Hydrometallurgy* **2019**, *185*, 149–161. [CrossRef]
35. Dahiya, S.; Tripathi, R.M.; Hegde, A.G. Biosorption of heavy metals and radionuclide from aqueous solutions by pre-treated arca shell biomass. *J. Hazard. Mater.* **2008**, *150*, 376–386. [CrossRef]
36. Xu, X.; Zou, J.; Zhao, X.-R.; Jiang, X.-Y.; Jiao, F.-P.; Yu, J.-G.; Liu, Q.; Teng, J. Facile assembly of three-dimensional cylindrical egg white embedded graphene oxide composite with good reusability for aqueous adsorption of rare earth elements. *Colloid Surface A* **2019**, *570*, 127–140. [CrossRef]
37. Zhang, S.; Kano, N.; Mishima, K.; Okawa, H. Adsorption and desorption mechanisms of rare earth elements (REEs) by layered double hydroxide (LDH) modified with chelating agents. *Appl. Sci.* **2019**, *9*, 4805. [CrossRef]
38. Shen, J.; Liang, C.; Zhong, J.; Xiao, M.; Zhou, J.; Liu, J.; Liu, J.; Ren, S. Adsorption behavior and mechanism of *Serratia marcescens* for Eu(III) in rare earth wastewater. *Environ. Sci. Pollut. Res.* **2021**, *28*, 56915–56926. [CrossRef]
39. Ghosh, S.B.; Bhattacharya, K.; Nayak, S.; Mukherjee, P.; Salaskar, D.; Kale, S.P. Identification of different species of *Bacillus* isolated from Nisargruna Biogas Plant by FTIR, UV-Vis and NIR spectroscopy. *Spectroc. Acta Part A-Mol. Biomol. Spectr.* **2015**, *148*, 420–426. [CrossRef]
40. Ngo-Thi, N.A.; Kirschner, C.; Naumann, D. Characterization and identification of microorganisms by FT-IR microspectrometry. *J. Mol. Struct.* **2003**, *661–662*, 371–380. [CrossRef]
41. Bombalska, A.; Mularczyk-Oliwa, M.; Kwasny, M.; Wlodarski, M.; Kaliszewski, M.; Kopczynski, K.; Szpakowska, M.; Trafny, E.A. Classification of the biological material with use of FTIR spectroscopy and statistical analysis. *Spectroc. Acta Part A-Mol. Biomol. Spectr.* **2011**, *78*, 1221–1226. [CrossRef] [PubMed]
42. Naumann, D.; Helm, D.; Labischinski, H. Microbiological characterizations by FT-IR spectroscopy. *Nature* **1991**, *351*, 81–82. [CrossRef] [PubMed]
43. Valentine, N.B.; Johnson, T.J.; Su, Y.F.; Forrester, J.B. FTIR spectroscopy for bacterial spore identification and classification. In Proceedings of the FTIR Spectroscopy for Bacterial Spore Identification and Classification, Boston, MA, USA, 31 December 2006; Volume 6378, p. 63780P.
44. Johnson, T.J.; Williams, S.D.; Valentine, N.B.; Su, Y.-F. The hydration number *n* of calcium dipicolinate trihydrate, CaDP·$n$H$_2$O, and its effect on the IR spectra of sporulated *Bacillus* bacteria. *Vib. Spectrosc.* **2010**, *53*, 28–33. [CrossRef]
45. Setlow, P. I will survive: DNA protection in bacterial spores. *Trends Microbiol.* **2007**, *15*, 172–180. [CrossRef]
46. Markai, S.; Andres, Y.; Montavon, G.; Grambow, B. Study of the interaction between europium(III) and *Bacillus subtilis*: Fixation sites, biosorption modeling and reversibility. *J. Colloid Interface Sci.* **2003**, *262*, 351–361. [CrossRef]
47. Martinez, R.E.; Pourret, O.; Takahashi, Y. Modeling of rare earth element sorption to the Gram positive *Bacillus subtilis* bacteria surface. *J. Colloid Interface Sci.* **2014**, *413*, 106–111. [CrossRef]
48. Ngwenya, B.T.; Mosselmans, J.F.W.; Magennis, M.; Atkinson, K.D.; Tourney, J.; Olive, V.; Ellam, R.M. Macroscopic and spectroscopic analysis of lanthanide adsorption to bacterial cells. *Geochim. Cosmochim. Acta* **2009**, *73*, 3134–3147. [CrossRef]
49. Moriwaki, H.; Koide, R.; Yoshikawa, R.; Warabino, Y.; Yamamoto, H. Adsorption of rare earth ions onto the cell walls of wild-type and lipoteichoic acid-defective strains of *Bacillus subtilis*. *Appl. Microbiol. Biotechnol.* **2013**, *97*, 3721–3728. [CrossRef]
50. Andres, Y.; MacCordick, H.J.; Hubert, J.-C. Adsorption of several actinide (Th, U) and lanthanide (La, Eu, Yb) ions by *Mycobacterium smegmatis*. *Appl. Microbiol. Biotechnol.* **1993**, *39*, 413–417. [CrossRef]
51. Bergsten-Torralba, L.R.; Nascimento, C.R.S.; Buss, D.F.; Giese, E.C. Kinetics and equilibrium study for the biosorption of lanthanum by *Penicillium simplicissimum INCQS 40,211*. *3 Biotech* **2021**, *11*, 460. [CrossRef]
52. da Costa, T.B.; Carlos da Silva, M.G.; Adeodato Vieira, M.G. Recovery of rare-earth metals from aqueous solutions by bio/adsorption using non-conventional materials: A review with recent studies and promising approaches in column applications. *J. Rare Earths* **2020**, *38*, 339–355. [CrossRef]
53. de Farias, A.B.V.; da Costa, T.B.; da Silva, M.G.C.; Vieira, M.G.A. Cerium recovery from aqueous solutions by bio/adsorption: A review in a circular economy context. *J. Clean. Prod.* **2021**, *326*, 129395. [CrossRef]

54. Moriwaki, H.; Masuda, R.; Yamazaki, Y.; Horiuchi, K.; Miyashita, M.; Kasahara, J.; Tanaka, T.; Yamamoto, H. Application of freeze-dried powders of genetically engineered microbial strains as adsorbents for rare earth metal ions. *ACS Appl. Mater. Interfaces* **2016**, *8*, 26524–26531. [CrossRef] [PubMed]
55. Shuster, B.; Khemmani, M.; Abe, K.; Huang, X.; Nakaya, Y.; Maryn, N.; Buttar, S.; Gonzalez, A.N.; Driks, A.; Sato, T.; et al. Contributions of crust proteins to spore surface properties in *Bacillus subtilis*. *Mol. Microbiol.* **2019**, *111*, 825–843. [CrossRef] [PubMed]